Supporting Information

A doping-adsorption-pyrolysis strategy for constructing atomically dispersed cobalt sites anchored on N-doped carbon framework as efficient bifunctional electrocatalyst for hydrogen evolution and oxygen reduction

Yuan Pan[a,b*], Minmin Wang[b] and Chao Feng[b*]

[a] Engineering Research Center for Waste Oil Recovery Technology and Equipment, Ministry of Education, Chongqing Technology and Business University, Chongqing 400067, China

[b] State Key Laboratory of Heavy Oil Processing, China University of Petroleum (East China), Qingdao 266580, Shandong, China

*Correspondence to: panyuan@upc.edu.cn (Y. Pan); fch_upc@163.com (C. Feng)

Experimental methods

Synthesis of Co SAs/CN-1: The methanol solution (150 mL) of dimethylimidazole (6.16 g) was slowly poured into the methanol solution (150 mL) of $Zn(NO_3)_2 \cdot 6H_2O$ (5.58 g) and $Co(NO_3)_2 \cdot 6H_2O$ (5.46 g) and mixed evenly. After stirring for 24 h, ZnCo@ZIF-8 was obtained after centrifugation, washing and vacuum drying (60°C, 10 h). Co SAs/CN-1 was obtained by pyrolysis ZnCo@ZIF-8 at 920°C in N_2 for 2 h.

Synthesis of Co SAs/CN-m (m=2, 3, 4): The DMF solution (50 mL) of 60 mg tetraphenylporphyrin cobalt was slowly added to DMF solution (50 mL) of ZnCo@ZIF-8 (0.25 g). After mixing and stirring for 24 h, and then centrifuged, washed and vacuum dried (60°C, 10 h) to obtain brown solid powder, denoted as ZnCo@ZIF-8@CoTPPx. Co SAs/CN-3-x was obtained by pyrolysis ZnCo@ZIF-8@CoTPPx at 920°C in N_2 for 2 h. x is the addition amount of tetraphenylporphyrin cobalt. When x is 50, 60 and 80 mg, the catalysts are denoted as Co SAs/CN-2, Co SAs/CN-3 and Co SAs/CN-4, respectively.

Characterization methods

X-ray diffraction test was performed with Panalytical X'pert PROX-ray diffractometer. Transmission electron microcopy was performed with a JEOL-2100F system. A Titan 80-300 scanning transmission electron microscope equipped with a probe spherical aberration corrector was used for high-angle dark field scanning transmission electron microscopy and energy loss spectroscopy, the working power was 300 kV. X-ray photoelectron spectroscopy measurements were carried out with ESCALABMK II. The N_2 adsorption/desorption analysis was performed at 77 K using a Micromeritics ASAP 2420 instrument. The specific surface area was determined by BET method, the microporous structure information was determined by HK method, and the mesoporous structure information was measured by BJH method. The X-ray absorption structure spectroscopic data were collected from Beijing Synchrotinometer Radiation Facility (BSRF) 1W1B station. The inductively coupled plasma (ICP-OES) spectra were obtained by ThermoScientific Icap 6300 ICP-OES.

Electrochemical measurements

The evaluation of HER performance of the catalyst was carried out on Shanghai Chenhua D type electrochemical workstation. A standard three-electrode system with 4 mm glassy carbon electrode as working electrode, graphite rod as counter electrode, Ag/AgCl electrode as reference

electrode in acidic condition and saturated calomel electrode (SCE) as reference electrode in alkaline condition was used for all performance evaluation. ORR performance was evaluated on PINE electrochemical workstation based on a three-electrode system, in which a rotating disk electrode (RDE) with a diameter of 5 mm was used as the reference electrode and platinum wire was used as the counter electrode.

The preparation method of the working electrode was as follows: 5 mg of synthetic material, 20 μL Nafion solution (5 wt%) and 1 mL ethanol were mixed and ultrasonic treated to obtain a ink. 20 μL of catalyst ink was uniformly dropped onto the working electrode and dried at room temperature. For HER test, linear sweep voltammetry (LSV) adopted a sweep speed of 5 mV·s^{-1}, and the electrolyte was 0.5 M H_2SO_4 and 1 M KOH, respectively. The electrochemical impedance (EIS) performance of the catalyst was tested in the frequency range of 100~0.1 kHz. For ORR test, LSV was tested in an oxygen-saturated 0.1 M KOH solution at a speed of 1600 rpm and a sweep speed of 5 mV·s^{-1}. All performance data were IR compensated and all measured potentials were corrected to reversible hydrogen electrode (RHE) potentials by the following conversion formula:

$$E(RHE) = E_{Ag/AgCl} + 0.197 + 0.059 \text{ pH},$$

$$E(RHE) = E_{SCE} + 0.241 + 0.059 \text{ pH}。$$

The calculation method of the number of active sites (n)：

$$n = \frac{Q}{2F} = \frac{I \cdot t}{2F} = \frac{I \cdot V / u}{2F}$$

The calculation method of conversion frequency (TOF, s^{-1}):

$$TOF = \frac{I}{mFn} = \frac{|j|A}{mFn}$$

Where, the total charge (Q) is obtained from the CV curve integral, I is the current (A), m is the number of electrons consumed to generate a H_2 molecule, and F is Faraday constant (96485 C mol^{-1}), t (s) is scanning time, V is the voltage (V), u for scanning speed (mV s^{-1}), |j| is current density, A is the area (m^2).

The number of electron transfer can be calculated by koutecky-Levich (K-L) equation:

$$\frac{1}{J} = \frac{1}{J_K} + \frac{1}{J_L} = \frac{1}{B\omega^{\frac{1}{2}}} + \frac{1}{J_K}$$

$$B = 0.62 nFC_o D_0^{\frac{2}{3}} V^{-\frac{1}{6}}$$

Where, J is the current density obtained by LSV curve, and J_L is the limiting current density,

J_K is the dynamic current density, ω is the angular velocity, F is Faraday constant, n is the number of electron transfer, C_0 is the volume concentration of oxygen (1.2×10^{-6} mol/cm^3), D_0 is the diffusion coefficient of oxygen (1.9×10^{-5} cm^2/s), V represents the kinematic viscosity of the electrolyte, B is the electron transfer rate constant.

Density functional theory calculations

The spin-polarized density functional theory (DFT) calculations used the Vienna ab initio simulation packages (VASP), and the generalized gradient approximation (GGA) with Perdew-Burke-Ernzerhof (PBE) functional was used to describe the exchange and correlation energy in all calculations[1]. The interactions between valence electrons and ionic cores is described by the projector-augmented wave (PAW) method. The plane wave cutoff energy was fixed at 400 eV. A graphene slab with Co and N atom substitution was built to model the CoN$_4$, thus obtaining the model with the lowest lattice mismatch in subsequent calculations. A 10 Å vacuum region to simulate the adsorption. All layers and the adsorbates were completely relaxed in all dimensions until the maximum force on a single atom was less than 0.03 eV Å^{-1} and the convergence of energy and forces was set to 1×10^{-4} Ha. The Brillouin region was sampled by the Monkhorst-Pack method with a $4 \times 4 \times 1$ k-point mesh.

For hydrogen evolution reaction (HER) in acid environment, the reaction Gibbs free energy ($\Delta G_H{}^*$) can be calculated as follows[2]:

$$\Delta G_H{}^* = \Delta E_H + \Delta E_{ZPE} - T\Delta S_H$$

where ΔE_H, ΔE_{ZPE}, and ΔS_H are the adsorption energy of hydrogen, the zero-point energy difference and the entropy difference. In standard conditions, $\Delta E_{ZPE} - T\Delta S_H$ is about 0.24 eV, hence ($\Delta G_H{}^*$) can be calculated by ΔE_H+0.24.

The (ORR) in alkali environment follows three elementary steps. The free energies of the intermediates at 298.15 K were obtained by:

$$\Delta G = \Delta E + \Delta E_{ZPE} - T\Delta S + eU$$

where ΔE_{ZPE}, ΔS and U are the zero-point energy changes, entropy changes and applied potentials. And ΔE is the binding energy of adsorption species HO*, O* and HOO*, with defined as follows:

$$\Delta E = E_{substrate + adsorbate} - E_{substrate} - E_{adsorbate}$$
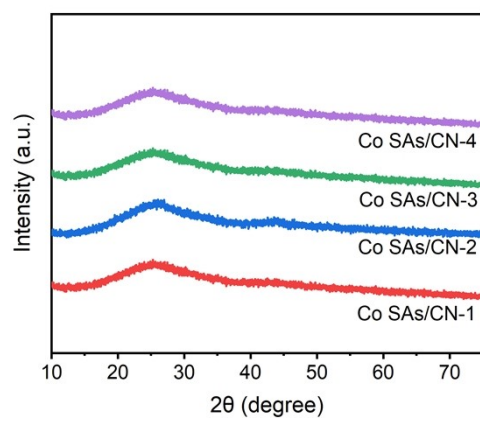
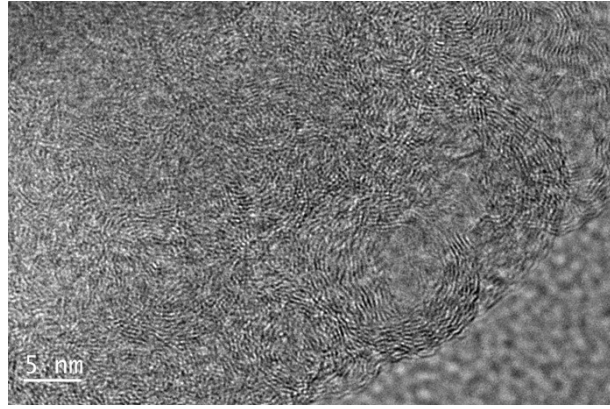Fig. S1 XRD patterns of the as-synthesized catalysts .

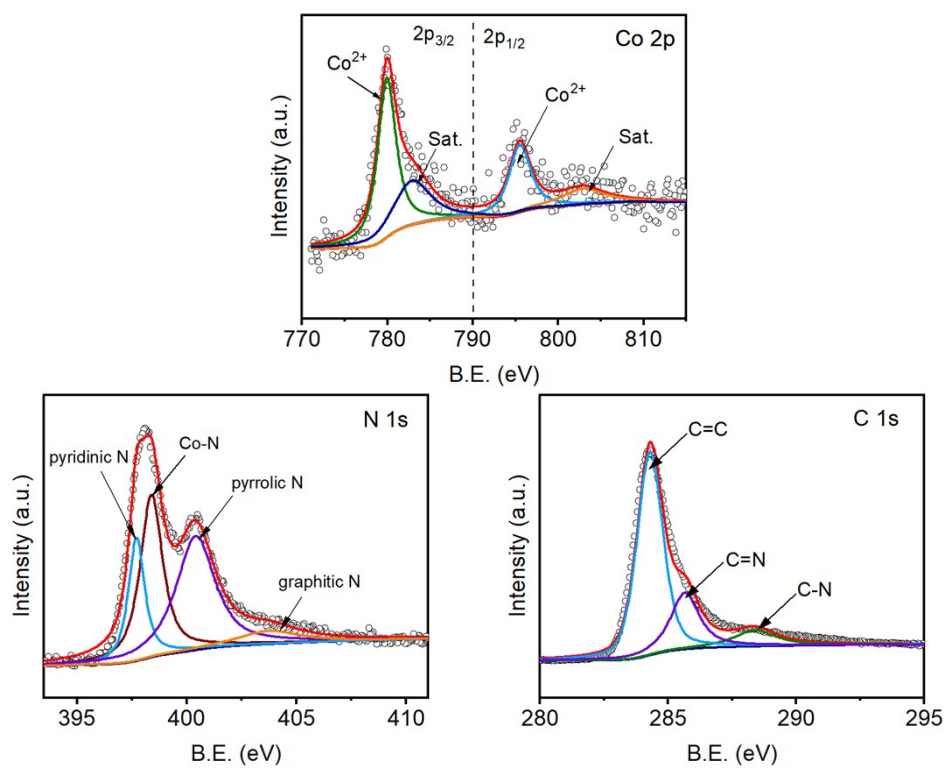Fig. S2 High-resolution TEM image of Co SAs/CN-3.

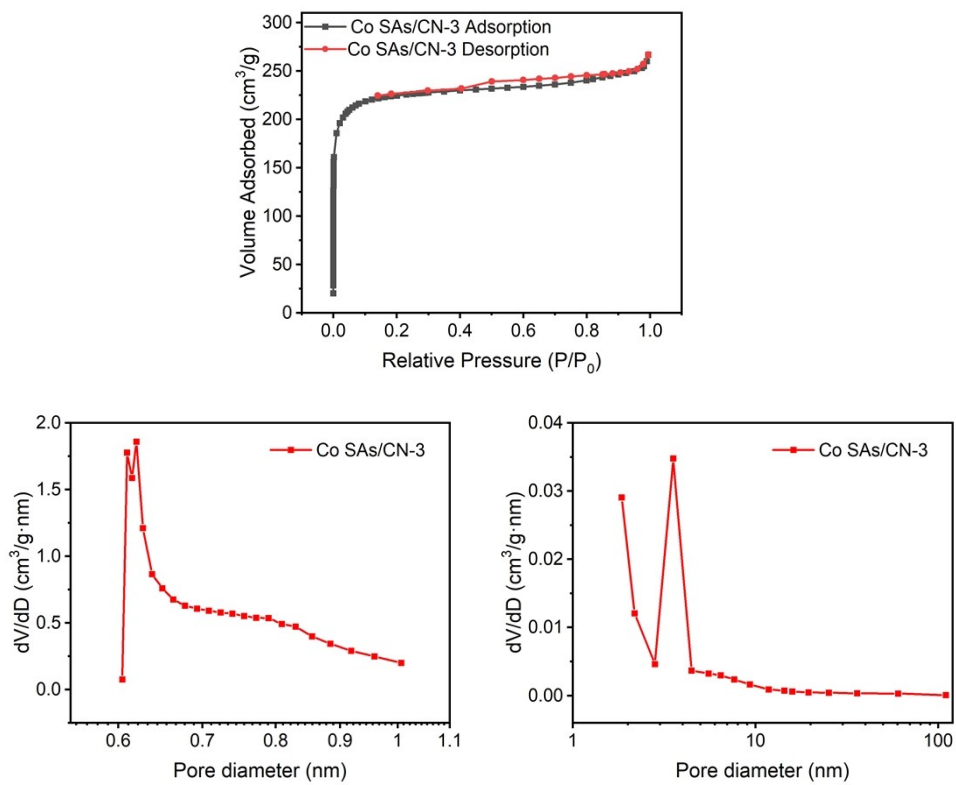Fig. S3 XPS spectra of Co SAs/CN-3 of (a) Co 2p, (b) N 1s, (c) C 1s.

Fig. S4 (a) N_2 adsorption-desorption isotherms, (b) micropore size distribution, (c)

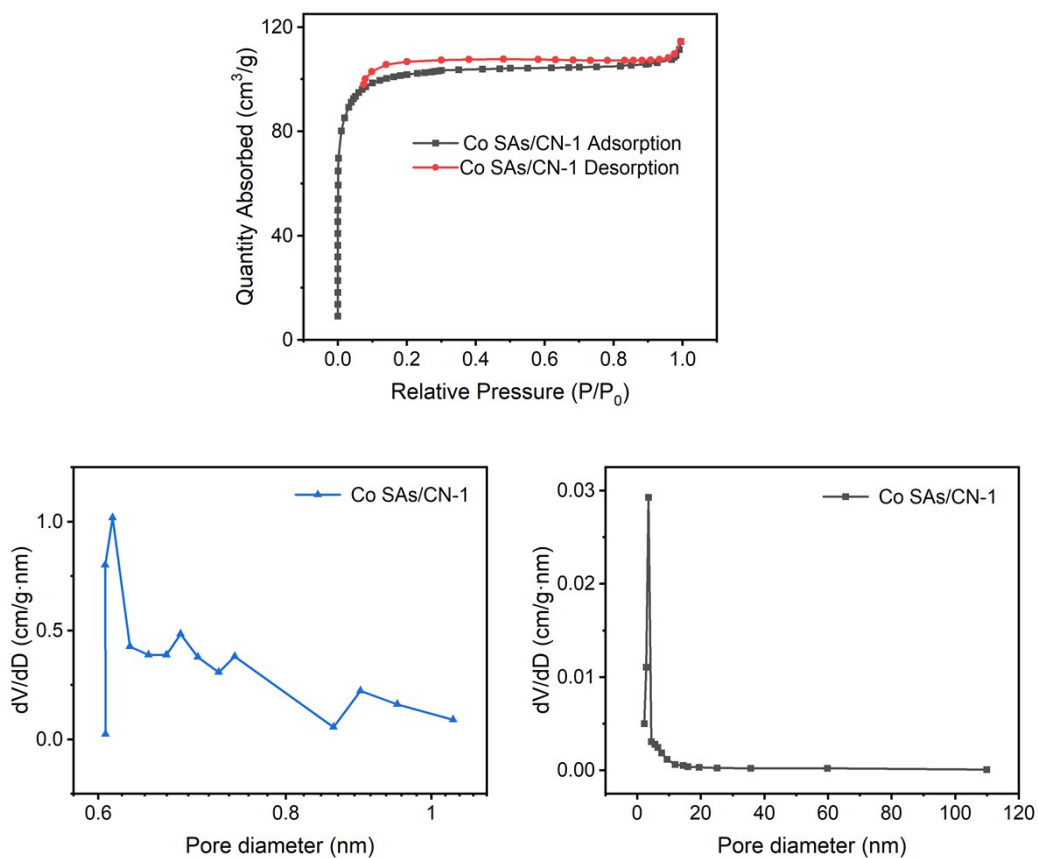mesoporous size distribution curves of Co SAs/CN-3.

Fig. S5 (a) N_2 adsorption-desorption isotherms, (b) micropore size distribution, (c)
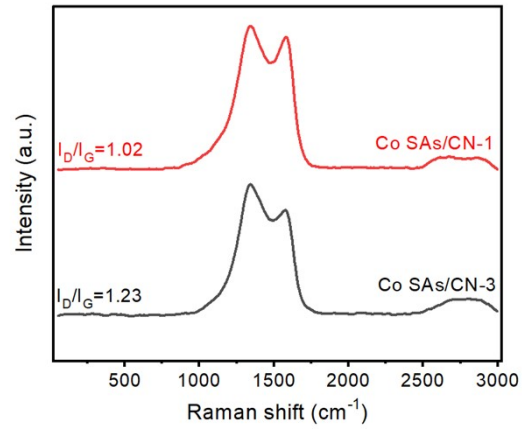
mesoporous size distribution curves of Co SAs/CN-1.

Fig. S6 Raman spectra of Co SAs/CN-1 and Co SAs/CN-3.
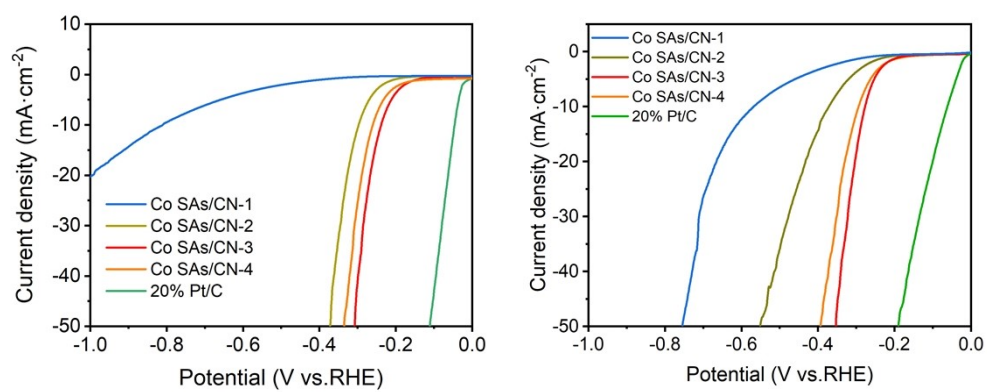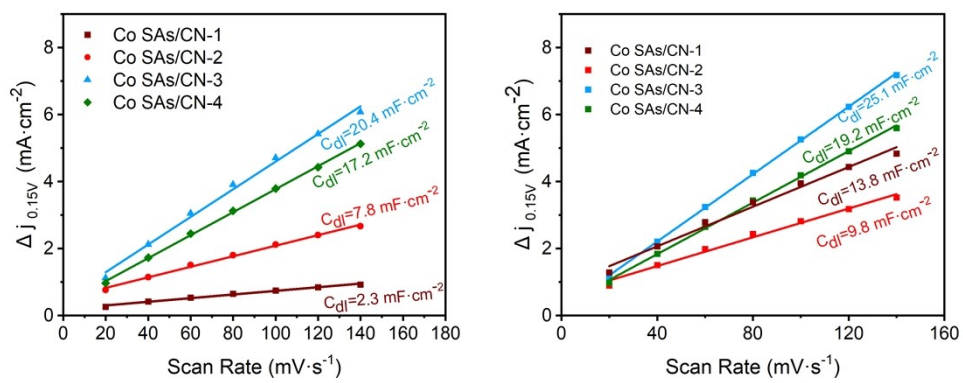
Fig. S7 LSV curves in (a) 0.5 M H_2SO_4, (b) 1 M KOH.

Fig. S8 C_{dl} curves of the as-synthesized catalysts in (a) 0.5 M H_2SO_4, (b) 1 M KOH for HER.
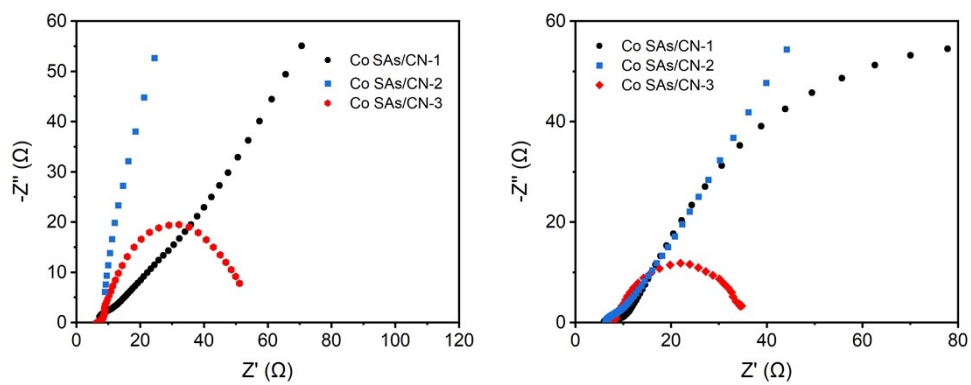
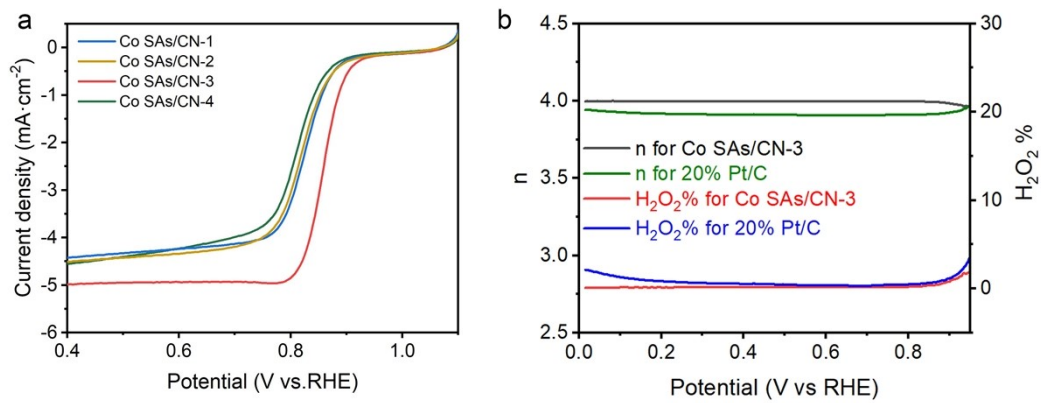Fig. S9 EIS curves of the as-synthesized catalysts in (a) 0.5 M H_2SO_4, (b) 1 M KOH for HER.

Fig. S10. (a) LSV curves of the as-synthesized catalysts in 0.1 M KOH for ORR, (b) H_2O_2 yield and electron transfer number of Co SAs/CN-3 and the commercial Pt/C.
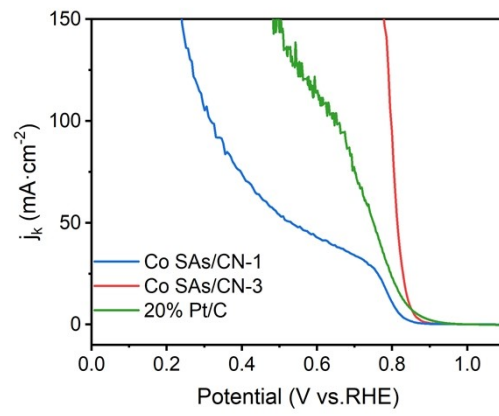
Fig. S11 j_k curves of the as-synthesized catalysts in 0.1 M KOH for ORR.
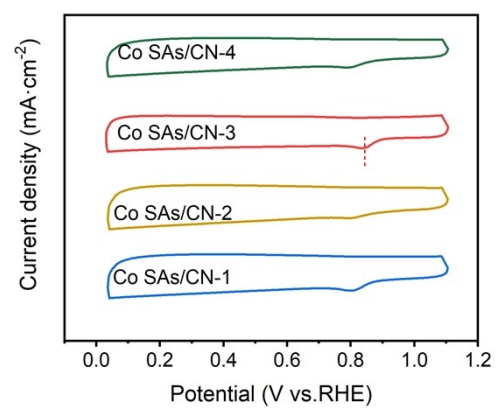
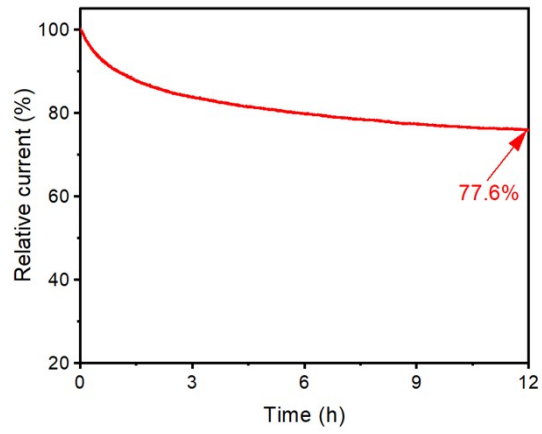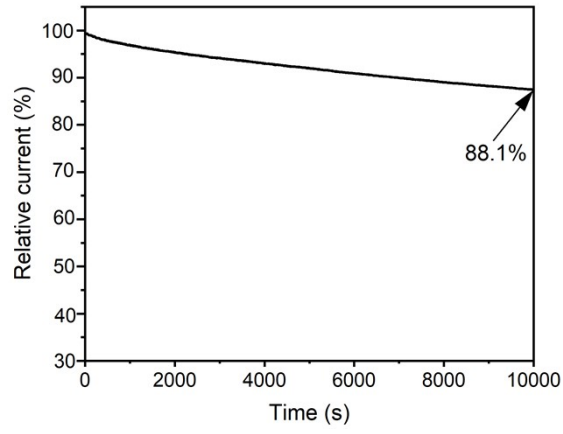Fig. S12 CV curves of the as-synthesized catalysts in 0.1 M KOH for ORR.

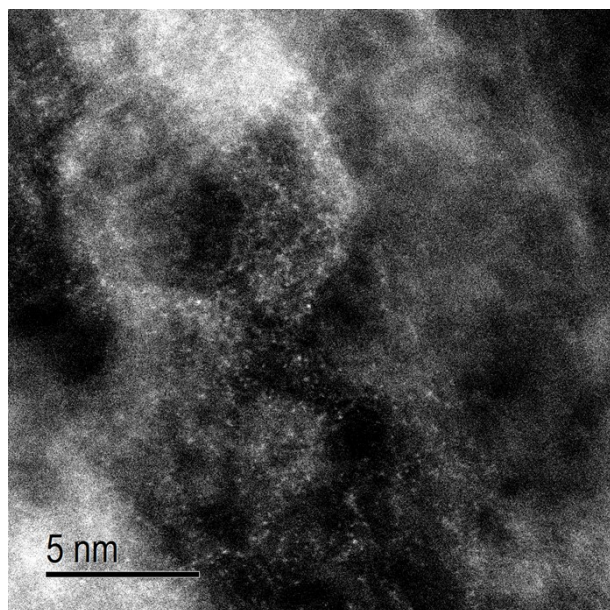Fig. S13 i-t curve of Co SAs/CN-3.

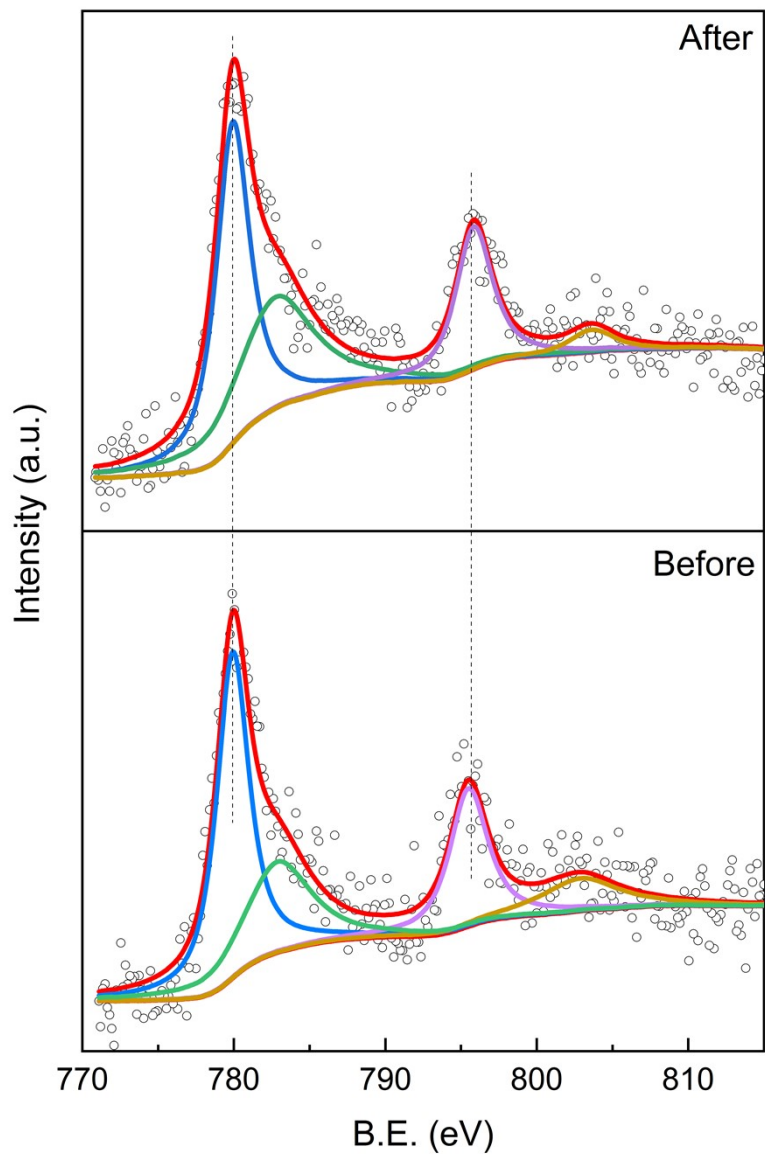Fig. S14 AC-HAADF-STEM image of Co SAs/CN-3 after 1000 cycles in 0.5 M H_2SO_4.

Fig. S15 Co 2p XPS spectra of Co SAs/CN-3 before and after 1000 cycles in 0.5 M H_2SO_4.
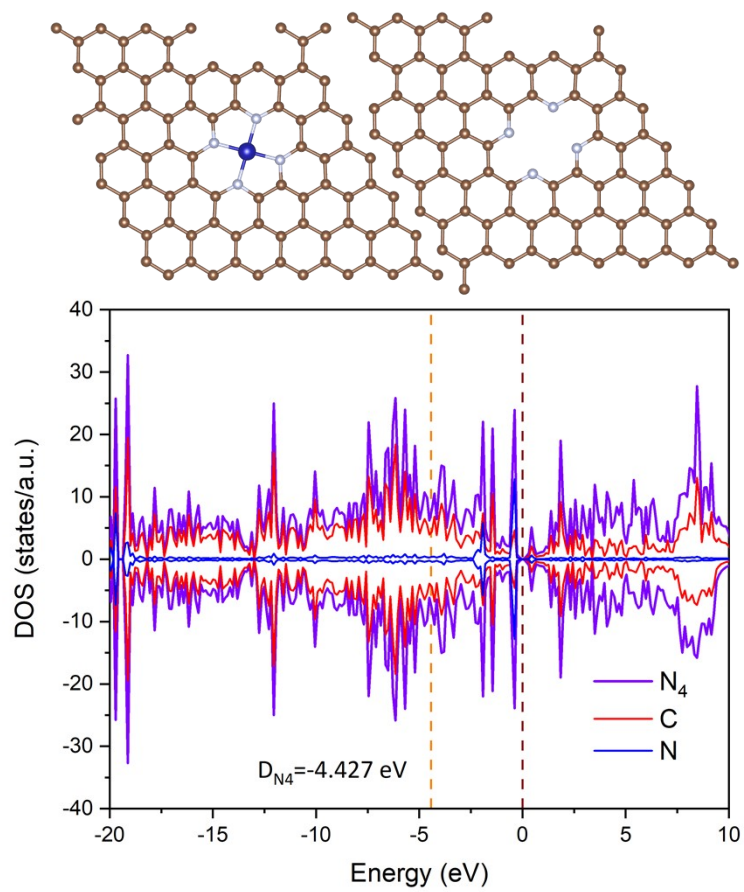
Fig. S16 (a) Structural model of CoN$_4$C and N$_4$C, (b) the DOS diagrams of N$_4$C.
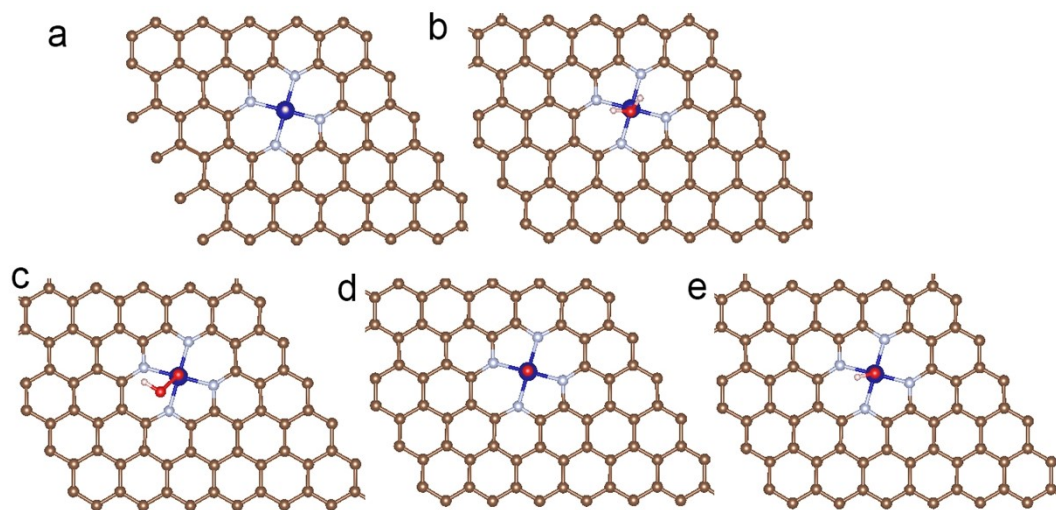
Fig. S17 Adsorbed state of reactant/intermediate species at active site, (a) H, (b) H_2O, (c) OOH, (d) O, (e) OH.

Table S1. EXAFS fitting parameters at the Co K-edge for various samples

Sample	Shell	N [a]	R (Å) [b]	σ^2 (Å$^2\cdot$10^{-3}) [c]	ΔE_0 (eV) [d]
Co SAs/CN-3	Co-N	4.3(5)	1.89(2)	6.7(7)	-5.1(6)

[a]N: coordination numbers; [b]R: bond distance; [c]σ^2: Debye-Waller factors; [d]ΔE_0: the inner potential correction. R factor: goodness of fit. S_0^2 was set as 0.80 for Co-N, which was obtained from the experimental EXAFS fit of reference CoPc by fixing CN as the known crystallographic value and was fixed to all the samples.

Table S2 Comparison of the electrocatalytic HER activity of Co SAs/CN-3 with other

representative electrocatalysts in 0.5 M H_2SO_4.

Catalyst	Electrolyte	η_{10} (mV vs. RHE)	Reference
Co SAs/CN-3	0.5 M H_2SO_4	238	This work.
$Mn_{0.05}Co_{0.95}Se_2$	0.5 M H_2SO_4	195	*J. Am. Chem. Soc.* 2016, 138, 5087.
Fe-Ni_3C-2%	0.5 M H_2SO_4	178	*Angew. Chem. Int. Ed.* 2017, 56, 1.
Co-NRCNTs	0.5 M H_2SO_4	260	*Angew. Chem. Int. Ed.* 2014, 53, 4372.
S_v-MoS_2 nanoflakes	0.5 M H_2SO_4	194	*Angew. Chem. Int. Ed.* 2019, 131, 2051.
Mo_2C/graphene	0.5 M H_2SO_4	237	*Adv. Mater.* 2017, 29, 1700072.
Co_9S_8@MoS_2	0.5 M H_2SO_4	190	*Adv. Mater.* 2015, 27, 4752.
CE-TaS_2	0.5 M H_2SO_4	192	*CrystEngComm* **2019**, *21*, 3517
Fe doped NiS_2	0.5 M H_2SO_4	198	*J. Mater. Chem. A* **2019**, *7*, 4971

Table S3 Comparison of the electrocatalytic HER activity of Co SAs/CN-3 with other representative electrocatalysts in 1 M KOH.

Catalyst	Electrolyte	η_{10} (mV vs. RHE)	Reference
Co SAs/CN-3	1 M KOH	278	This work.
Co₃O₄/MoS₂	1 M KOH	205	*Appl. Catal. B- Environ.* 2019, *248,* 202
Mo₂C-NCNTs	1 M KOH	257	*J. Mater. Chem. A* 2015, *3,* 5783
Co-PNCNFs	1 M KOH	249	*J. Mater. Chem. A* 2016, *4,* 12818
CoOx@CN	1 M KOH	232	*J. Am. Chem. Soc.* 2015, *137,* 15753
Ni₂₋ₓCoₓP	1 M KOH	209	*Adv. Funct. Mater.* 2016, 26, 6785.
Co/CoP	1 M KOH	253	*Adv. Energy Mater.* 2017, 7, 1602355.
Co₉S₈@NOSC	1 M KOH	320	*Adv. Funct. Mater.* 2017, 27, 1606585.
O-CoSe₂/CC orthorhombic phase	1 M KOH	270	*Adv. Mater.* 2016, 28, 7527.
Co₂B-500	1 M KOH	328	*Adv. Energy Mater.* 2016, 6, 1502313..
Ni₃S₂/Nickel Foam	1 M KOH	310	*Adv. Funct. Mater.* 2016, 26, 4661.

Table S4 Comparison of the electrocatalytic ORR activity of Co SAs/CN-3 with other

representative electrocatalysts.

Catalyst	Electrolyte	$E_{1/2}$ (V vs. RHE)	Reference
Co SAs/CN-3	0.1 M KOH	0.87	This work.
Fe$_3$C@N-CNT	0.1 M KOH	0.85	*Energy Environ. Sci.* 2016, 9, 3092-3096.
Co−N/CNFs	0.1 M KOH	0.82	*ACS Catal.* 2017, 7, 6864-6871.
Fe@Aza-PON	0.1 M KOH	0.839	*J. Am. Chem. Soc.* 2018, 140, 1737-1742.
CNT/PC	0.1 M KOH	0.88	*J. Am. Chem. Soc.* 2016, 138, 15046.
C-MOF-C2-900	0.1 M KOH	0.82	*Adv. Mater.* 2018, 30, 1705431.
D-AC@2Mn-4Co	0.1 M KOH	0.792	*Adv. Mater.* 2016, 28, 8771.
S,N-Fe/N/CCNT	0.1 M KOH	0.85	*Angew. Chem. Int. Ed.* 2017, 56, 610.
Co-ISAS/p-CN	0.1 M KOH	0.838	*Adv. Mater.* 2018, 1706508.
Co@Co$_3$O$_4$/NC-1	0.1 M KOH	0.80	*Angew. Chem. Int. Ed.* 2016, 55, 4087-4091.

References

1. R. Zhang, P. Li, R. Xiao, N. Liu, B. *Chen, Appl.Catal. B: Environ.,* 2016, **196**, 142-154.

2. K. Sun, Y. Liu, Y. Pan, H. Zhu, J. Zhao, L. Zeng, Z. Liu, C. Liu, *Nano Research*, 2018, **11** , 4368-4379.